ACADEMIC PRESS

Available online at www.sciencedirect.com
SCIENCE DIRECT®

Journal of Catalysis 217 (2003) 107–116

JOURNAL OF CATALYSIS

www.elsevier.com/locate/jcat

Selective N,N-methylation of aniline over cocrystallized zeolites RHO and zeolite X (FAU) and over Linde type L (Sr,K-LTL)

L.J. Garces,[a] V.D. Makwana,[b] B. Hincapie,[a] A. Sacco,[d] and S.L. Suib [a,b,c,*]

[a] *Institute of Materials Science, University of Connecticut, Storrs, CT 06269, USA*
[b] *Department of Chemistry, U-60, University of Connecticut, Storrs, CT 06269-3060, USA*
[c] *Department of Chemical Engineering, University of Connecticut, Storrs, CT 06269, USA*
[d] *Department of Chemical Engineering, Northeastern University, 342 Snell Engineering, Boston, MA 02115, USA*

Received 9 September 2002; revised 27 January 2003; accepted 29 January 2003

Abstract

Alkylation of aniline ($PhNH_2$) with methanol (MeOH) over cocrystallized zeolite RHO–zeolite X (FAU) and over zeolite Linde type L (Sr,K-LTL) as catalysts has been studied. Cocrystallized zeolite RHO–zeolite X (FAU) favors the formation of *N*,*N*-dimethylaniline (NNDMA) with high selectivity > 90%, having an advantage over pure zeolite X (FAU) of staying active even after 10 h of reaction. Activity of cocrystallized RHO–zeolite X (FAU) is higher than that for Sr,K-LTL in terms of the production of *N*,*N*-dimethylaniline.

Keywords: Aniline; Methylation; Cocrystallized zeolites; Zeolite RHO; Zeolite LTL; Zeolite X; *N*,*N*-Dimethylaniline

1. Introduction

Synthesis of *N*,*N*-dimethylaniline (NNDMA) is an industrially important process due to its use as a raw material in organic syntheses as well as its role as an intermediate in dye-stuff production and in the pharmaceutical and agrochemical industries [1]. The gas-phase reaction involving the alkylation of aniline ($PhNH_2$) with methanol (MeOH) has been previously studied using several different kinds of materials such as clays, zeolites, and composites. Layered double hydroxides (LDH) known as hydrotalcites (HT) containing magnesium and aluminum have also been studied for this reaction with the formation of only a single product (*N*-methylaniline) [2]. In the case of ZSM-5, the extent of conversion using this material increases with increasing aluminum content [3]. This reaction has been catalyzed using AlPO4-5, AlPO4-11, CoAPO-5, CoAPO-11, ZAPO-5, and ZAPO-11 with the formation of *N*-methylaniline (N-MA), *N*,*N*-dimethylaniline, and *N*-methyltoluidine (N-MT) where the product distribution has been found to be influenced by the space velocity and the aniline to methanol ratio as well as the acidity of the catalyst [4].

N-methylation products have been reported as being predominant over Al-HMS mesoporous molecular sieves [5]. Oxides such as γ-alumina have also been used with N-methylation being the predominant reaction product [6]. Vanadium-incorporated aluminophosphate molecular sieves (VAPO-5 and VAPO-11) lead to the selective formation of *N*-methylaniline and *N*,*N*-dimethylaniline [7]. High selectivity to *N*-methylaniline is obtained over metallosilicates [8]. N-Methylation of aniline with methanol over MgO catalysts has also been reported [9]. Zeolites X and Y ion-exchanged with Li, Na, K, Rb, and Cs also have been used for this reaction. NNDMA is produced mainly over zeolite X. NMA is produced over zeolite Y. A mixture of N and C methylated products can be obtained over the more acidic form of the zeolites. A rapid deactivation of zeolite X (completely deactivated in 6 h) has been reported [10].

In this work the synthesis of *N*,*N*-dimethylaniline from methanol and aniline over cocrystallized RHO and X (FAU) zeolites and over Linde type L (Sr,K-LTL) zeolite is reported. We have studied effect of the different zeolite X to zeolite RHO ratios on the activity and selectivity of the gas-phase reaction involving alkylation of aniline with methanol. To the best of our knowledge there are no previous reports of the use of cocrystallized zeolites and Sr, K-LTL as catalysts for this reaction.

* Corresponding author.
E-mail address: suib@uconnvm.uconn.edu (S.L. Suib).

0021-9517/03/$ – see front matter
doi:10.1016/S0021-9517(03)00048-4

Zeolite RHO is a small pore size zeolite, 3.6×3.6 Å with a low Si/Al ratio (2.5–3.0). Cesium hydroxide is required for the preparation of zeolite RHO [11,12]. When a very small amount of Cs is used in the synthesis of zeolite RHO, zeolite X (FAU) will be formed as one of the products [11]. When Cs is not uniformly distributed in the gel, some zeolite X (FAU) will also be formed. Usually this is not a result expected in the synthesis of zeolite RHO, but in this case advantage of that result was taken to test the synergetic effect of the cocrystallized zeolite X (FAU) and zeolite RHO in the reaction between MeOH and $PhNH_2$.

Zeolite RHO is very selective for the production of dimethylamine [13]. Zeolite RHO can activate methanol for alkylation of amines but the aniline molecule, compared to ammonia, is too big to fit inside the pores of zeolite RHO. Pure alkaline zeolite X is a selective catalyst for the production of NNDMA and adsorbs aniline but deactivates in a short period of time. We expect that the use of these cocrystallized zeolites will increase the selectivity to NNDMA and stay active for longer time.

Industrial syntheses of both zeolites independently could be more expensive and difficult to handle because this involves two different synthetic processes. Thus the possibility of cocrystallizing both zeolites is economically attractive, due to enhanced stability of the catalyst.

2. Experimental

2.1. Synthesis of catalysts

2.1.1. Synthesis of cocrystallized RHO–zeolite X (FAU) catalysts

Cocrystallized zeolite RHO with zeolite X (FAU) was synthesized by dissolving sodium aluminate (EM Science, 85.53%) in double-deionized water and then adding sodium hydroxide (Alfa Aesar, 97%). This basic solution was mixed with cesium hydroxide (Aldrich, 99.9%, 50% wt in water) and colloidal silica (Ludox LS-30 Aldrich 30%). The batch compositions used to prepare these materials are shown in Table 1. All of the gels were stirred using a magnetic bar overnight and then aged for 6 days at room temperature. The crystallization was carried out at 85 °C for 72 h. The product was washed with double-deionized water until the pH was less than 9 and then dried overnight at 100 °C. XRD analyses were performed immediately after drying.

Table 1
Batch composition of the prepared zeolites

Catalyst	Batch Composition (molar ratio)				
(zeolite)	Na_2O	Cs_2O	Al_2O_3	SiO_2	H_2O
C-18 (FAU/RHO)	3.3	0.44	1	12	134.3
C-19 (FAU/RHO)	3.9	0.51	1	14	156.7
C-20 (FAU/RHO)	4.4	0.59	1	16	179.2
C-11-1 (RHO)	3.0	0.4	1	10.8	121.1
	K_2O	SrO	Al_2O_3	SiO_2	H_2O
C-LTL (LTL)	2.3	0.1	1	10	160

2.1.2. Synthesis of Linde type L catalyst

Zeolite LTL was synthesized by hydrothermal crystallization of a gel at 150 °C during 230 h. The gel was produced by mixing solutions 1 and 2, prepared as follows:

1. 2.5 g of aluminum hydroxide $Al(OH)_3$ (Aldrich, Lot 10809 BU, % Al_2O_3 51.7%) was dissolved in a solution of 3.71 g of potassium hydroxide (J.T. Baker, Lot. M 12917, 87.6%) and 6.18 g of double-deionized water (DDW);
2. 0.35 g of strontium hydroxide octahydrate (Aldrich, Lot 01517 JR 95%) were dissolved in 9.35 g DDW and the resulting solution was added to 14.5 mL of colloidal silica HS-40 (Aldrich, Lot 14007 Lu, 39.9%).

The batch composition of the gel formed is reported in Table 1.

2.2. Characterization of catalysts

2.2.1. X-ray diffraction (XRD)

The zeolites were characterized by X-ray diffraction using a Scintag XDS-200 powder diffractometer on finely powdered samples using Cu-K_α radiation and 45 kV and 40 mA. The scans were done at 2° per minute. The XRD patterns were recorded for 2θ's between 5 and 40° and the phases were identified using a JCPDS database. The diffraction pattern for zeolite RHO was compared to data published in the literature [12].

An X-ray calibration curve was prepared by mixing pure zeolite RHO and zeolite X (FAU) in known amounts. The intensity ratios of the 8.264°, 2θ line for zeolite RHO and the 6.03° 2θ line for zeolite X (FAU), were used to determine the FAU/RHO ratio in the actual catalysts.

2.2.2. Field emission scanning electron microscopy (FESEM)

Particle size and morphology were determined on a Zeiss DSM 982 Gemini field emission scanning electron microscope (FESEM) with a Schottky emiter at an acceleratinge voltage of 2 kV with a beam current of about 1 μA.

2.2.3. Chemical composition by EDX and ICP

An ECON IV energy dispersive X-ray (EDX) analyzer Model 9800 was used for EDX studies. An average of three analyses was done to calculate average concentrations and chemical compositions. Samples for ICP analyses were prepared by dissolving 0.2 g of sample in approximately 10 mL of HF and then diluting to 100 mL with DDW. Inductively coupled plasma optical emission spectrometry was done in a Perkin-Elmer P-40 with AS 60 autosampler.

2.2.4. Surface area (BET)

A Micromeritics ASAP 2010 equipped with an ASAP 2010 V4 software was used for surface area determinations. About 0.1 g of sample was loaded into the glass sample bulb and degassed at 400 °C for 4 h. The surface area of the samples was obtained using the Brunauer–Emmett–Teller (BET) model.

2.2.5. Fourier transform infrared spectra (FTIR)

FTIR experiments were done on a Nicolet Magna IR system 750 FT-IR spectrometer with a resolution of 4 cm^{-1}. KBr pellets of the catalysts were analyzed in the range 4000–400 cm^{-1}.

2.2.6. Aniline adsorption

In order to determine the capacity of the catalyst to adsorb aniline a method described in Ref. [14] was followed. The amount of aniline needed to yield a monolayer coverage on the solid (X_m) can be related to the degree of acidity of the catalyst. This quantity was determined for aniline at a wavelength of 234 nm by UV–Vis spectrophotometry using a Hewlett-Packard 8452A diode array spectrophotometer and applying the Langmuir equation [14].

2.3. Catalytic studies

The reactions were performed in a tubular quartz reactor packed with 50 mg of the desired catalyst. The reactor was heated to the desired temperature using a tubular furnace and the temperature was measured at the middle of the catalyst bed using a digital temperature controller. The catalyst was pretreated at 450 °C in a flow of helium for 5 h. After pretreatment the samples were cooled down to 400 °C, the reaction temperature. Aniline and methanol in a 1:3.5 ratio were introduced simultaneously into the system. Two different bubblers were used for the reactants and He (UHP, Airgas) was the carrier gas. This feed ratio of the reactants was controlled by varying the carrier gas flow rate.

The reactor outlet was connected to a Hewlett-Packard 5890 Series II gas chromatograph equipped with a gas sampling valve. A Carbowax SLP CW-20M capillary column, 25 m long and 0.5 μm internal diameter, was used for the separation of the products. After 1 h of reaction a sample was taken and injected into a gas chromatography–mass spectrometry (GC-MS). This way the products were identified. The product was also identified with a GC/FID using a commercially available sample of *N*,*N*-dimethylaniline. All materials listed in Table 1 were used under the same conditions described above. A blank run without any catalyst was also carried out as the baseline. No reaction was observed in this case.

2.3.1. Gas chromatography–mass spectrometry

Gas chromatography–mass spectrometry of the product mixtures was performed in a Hewlett-Packard Model 5890. A sample was taken after 1 h of reaction and injected to the GC-MS for identification of the products.

3. Results

3.1. Characterization of catalysts

3.1.1. X-ray diffraction (XRD)

The XRD patterns confirmed zeolites RHO and zeolite X (FAU) as the only phases present for the cocrystallized materials (Fig. 1) and zeolite LTL (Fig. 2). In the case of cocrystallized RHO–zeolite X (FAU) the X-ray pattern showed the 8.36, 14.56, 25.67, 27.03, 28.47, and 29.78°, 2θ line characteristic of zeolite RHO as well as the 6.03° 2θ line for zeolite X (FAU). The sample labeled as C-20 showed peaks characteristic of completely dehydrated and partially

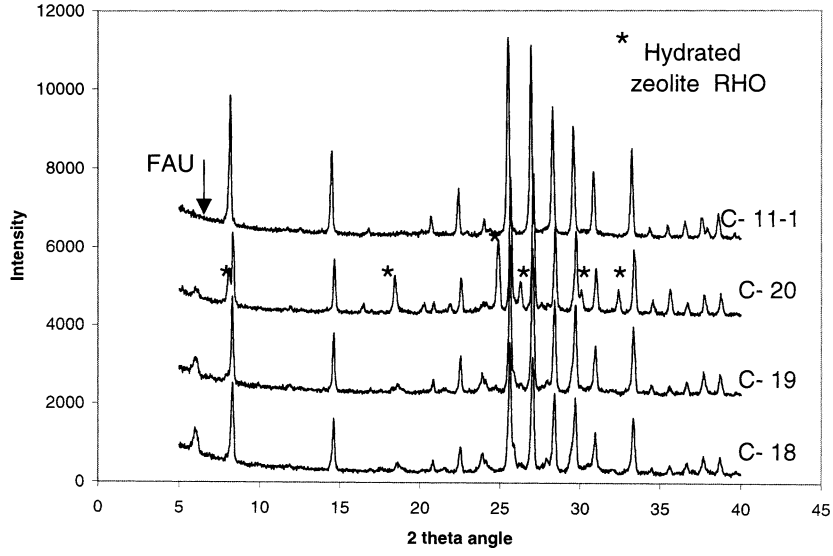

Fig. 1. X-ray diffraction patterns for cocrystallized zeolite RHO–zeolite X (FAU).

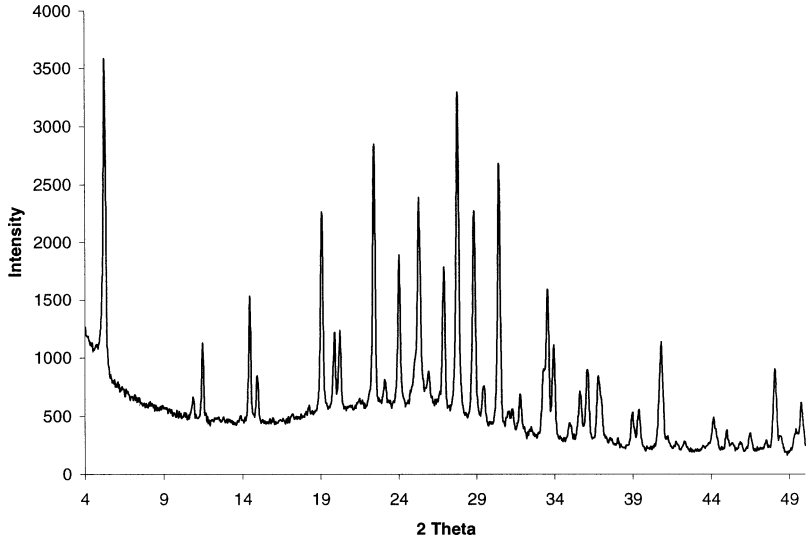

Fig. 2. X-ray diffraction pattern of zeolite LTL.

Table 2
Composition of synthesized catalysts

Catalyst	FAU/RHO ratio	SiO_2/Al_2O_3 molar ratio		$(Na_2O + Cs_2O)/SiO_2$ molar ratio	
	(XRD)	EDX	ICP	EDX	ICP
C-18	0.214	3.75	5.81	0.142	0.104
C-19	0.131	3.94	4.64	0.140	0.156
C-20	0.093	4.04	6.0	0.108	0.111
C-11-1	0.001	3.68	3.97	0.189	0.160
C-LTL	0	5.4	5.81	0.165[a]	0.08[a]

[a] $(K_2O + SrO)/SiO_2$ molar ratio.

dehydrated zeolite RHO and also the peak for zeolite X (FAU). Zeolite Linde type L showed the 5.26, 18.98, 22.33, 25.21, 27.69, 28.74, and 30.35° 2θ lines characteristic of this material. The FAU/RHO ratio for the cocrystallized RHO–zeolite X (FAU) was calculated by relating the intensity of the 8.36° 2θ line for RHO with the intensity of the 6.03° 2θ line for zeolite X (FAU) and relating them to a standard quantification curve that was developed by preparing several mixtures of RHO and FAU. An X-ray calibration curve was developed with these standards and used to calculate the FAU/RHO ratio in the actual samples as described above. The FAU/RHO ratio calculated using this curve is reported in Table 2.

3.1.2. Field emission scanning electron microscopy

The shapes of the zeolites (see Fig. 3) correspond to similar morphologies reported in the literature. Zeolite Sr,K,LTL is cylindrical [15], and zeolite RHO is dodecahedral in shape [16]. Another phase observed in the SEM pictures of the cocrystallized zeolites has the shape of flat discs. In all cases the crystal size of this phase which must correspond to zeolite X (FAU) is constant. For C-11-1 no discs were observed. The amount of the disc-shaped phase was higher in C-18, less for C-19, and even lower for C-20. The size of the particles increases in this sequence C-11-1 < C-18 < C-19 < C-20 as reported in Table 3.

3.1.3. EDX and ICP

Table 2 shows that the main elements for the catalysts studied herein are silicon, aluminum, cesium, and sodium in the case of cocrystallized RHO–zeolite X (FAU) and silicon, aluminum, sodium, strontium, and potassium in the case of zeolite LTL. There are some differences in the values obtained using both techniques. The size of the sample for EDX is smaller since SEM was used to select the area of analysis. For catalysts 18 and 20 the SiO_2/Al_2O_3 ratio obtained by ICP is larger than expected. There may be some amorphous silica that can make the ICP value higher. EDX analysis was performed by SEM on crystalline material.

3.1.4. Surface area (BET)

Table 3 shows surface areas for the catalysts studied. In the case of surface areas for the series of cocrystallized zeolite RHO–zeolite X (FAU) there is a direct relationship between the rate of formation of NNDMA and the value for the surface area. In the case of zeolite LTL, even though the surface area was very large compared to others, the activity of the catalysts is very poor (see Discussion).

The surface area for the cocrystallized zeolites is also related to the concentration of zeolite X (FAU). C-18 with the highest FAU/RHO ratio also had the highest surface area. The low surface area for C-11-1 may be due to framework distortion caused by loss of water during the pretreatment of the sample, similar to reaction conditions.

3.1.5. Fourier transform infrared spectra

From Fig. 4 there are other phases present in C-18 besides zeolite RHO. There is a broadening of the band around 1043 cm^{-1}, that is not present in the spectrum for the pure phase C-11-1. Around 600 cm^{-1} for C-18 and C-19 there

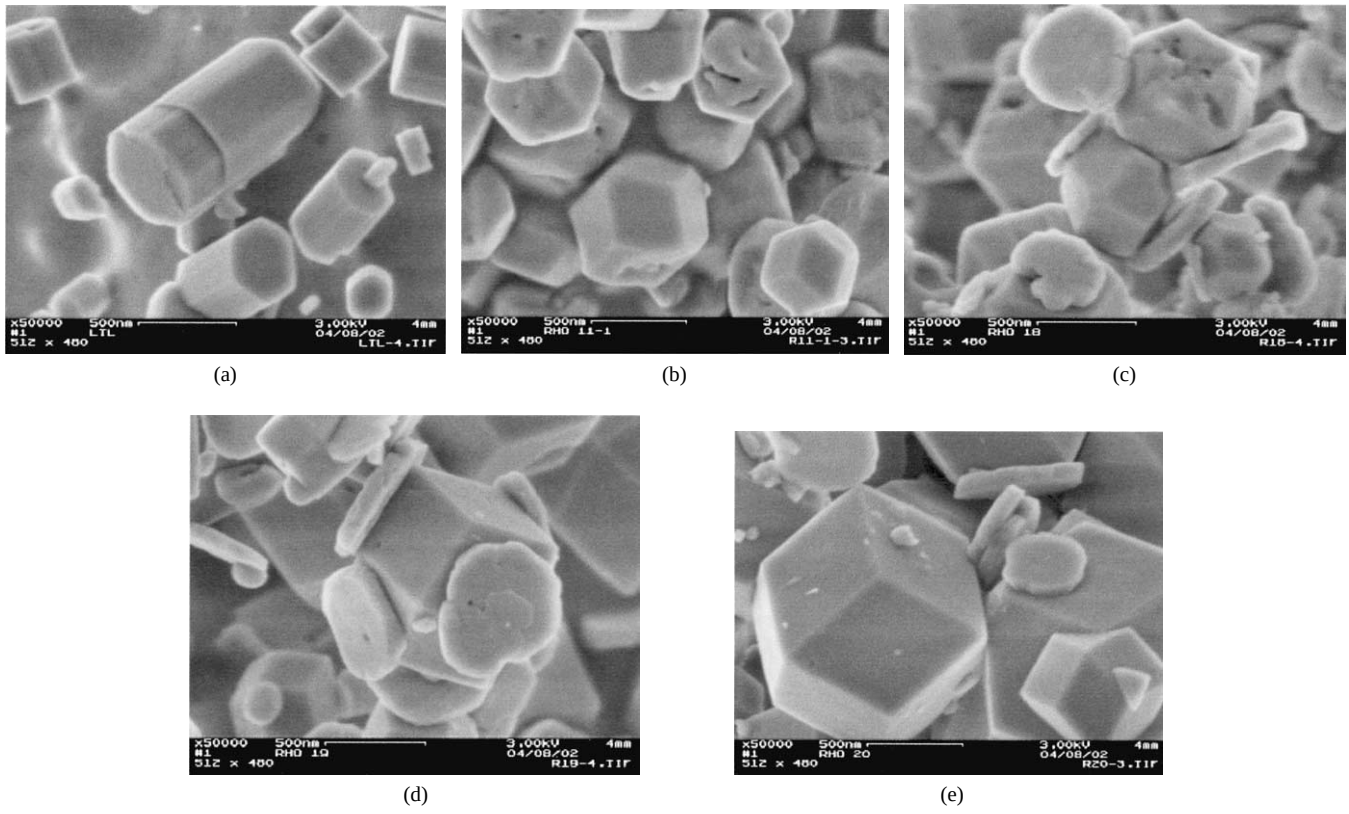

(a) (b) (c)

(d) (e)

Fig. 3. FESEM of catalysts. (a) C-LTL, (b) C-11-1, (c) C-18, (d) C-19, and (e) C-20.

Table 3
Surface area and particle size of catalysts

Catalyst	Surface area (m^2/g) by BET	Median pore diameter (Å)	Particle size (μm) by FESEM
C-18	92.29 ± 3.04	19.9	0.73
C-19	70.02 ± 2.38	7.2	1.05
C-20	25.17 ± 1.04	6.5	1.37
C-11-1	17.20 ± 0.69	863.3	0.68
C-LTL	213.16 ± 7.31	4.9	1.1×0.43

C-18–20: zeolite X (FAU) has the shape of a disc with length 0.65 μm and thickness 0.1 μm.

are very small bands that are not present in the spectra for catalysts 11-1 and 20 (low FAU content).

The displacement of the band around 796.5 cm^{-1} has been previously related to different Si/Al ratios for these zeolites. For higher values of the IR frequencies of this band the Si/Al ratio is also higher [17]. A comparison between FTIR data for C-11-1 (pure RHO) before and after reaction is presented in Fig. 5. There is a small difference, in the region 3000–2000 cm^{-1} for samples before and after reaction. The C-11-1 after reaction shows some bands in this region that can be associated with $–CH_2$ vibrations. After subtracting both spectra a good match with that for formate species is obtained.

The FTIR spectra for C-LTL before and after reaction are presented in Fig. 6. There is not an appreciable difference in these two spectra. The bands around 3000–2000 cm^{-1} observed in the spectrum for C-11-1 after reaction were not detected for LTL samples.

3.1.6. Aniline adsorption

From the results of aniline adsorption for the different catalysts shown in Table 4, the higher adsorption represented in the higher X_m values (base adsorbed in a monolayer) is for catalysts labeled C-18 followed by LTL, C-19, C-11-1, and C-20. For the materials with the largest surface area, the X_m value was also highest. This was true for materials of similar composition (C-18–20). This is not the case for LTL which has the highest surface area but aniline adsorption is not the greatest.

3.2. Catalysis

NNDMA was identified as the only product in all alkylation reactions by GC-FID (comparing retention time against commercial sample) and by GC-MS. The percentage of conversion was calculated based on aniline [18]. From Fig. 7, all catalysts during the first minutes of the reaction show that some aniline is still unreacted. After approximately 20 min, differences among the catalysts start to emerge. When C-18 was used, the highest aniline conversion was obtained ($\sim$ 95%) and the activity of the catalyst was the same over the reaction period (10 h). The same behavior was observed for C-19, but the conversion of aniline was approximately 10% less than the conversion when C-18 was used ($\sim$ 85%).

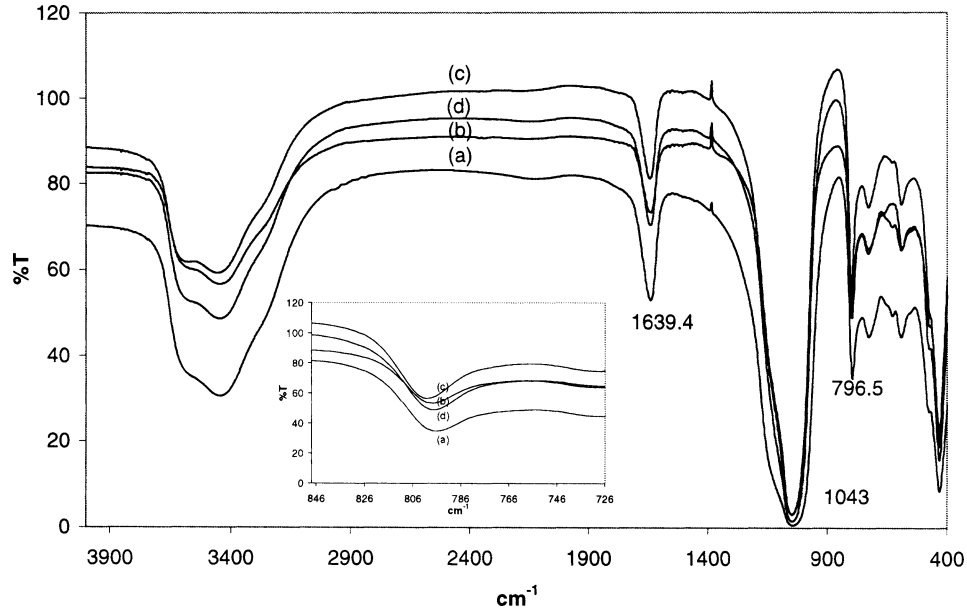

Fig. 4. FTIR of cocrystallized zeolite RHO–zeolite X (FAU). (a) C-18, (b) C-19, (c) C-20, and (d) C-11-1.

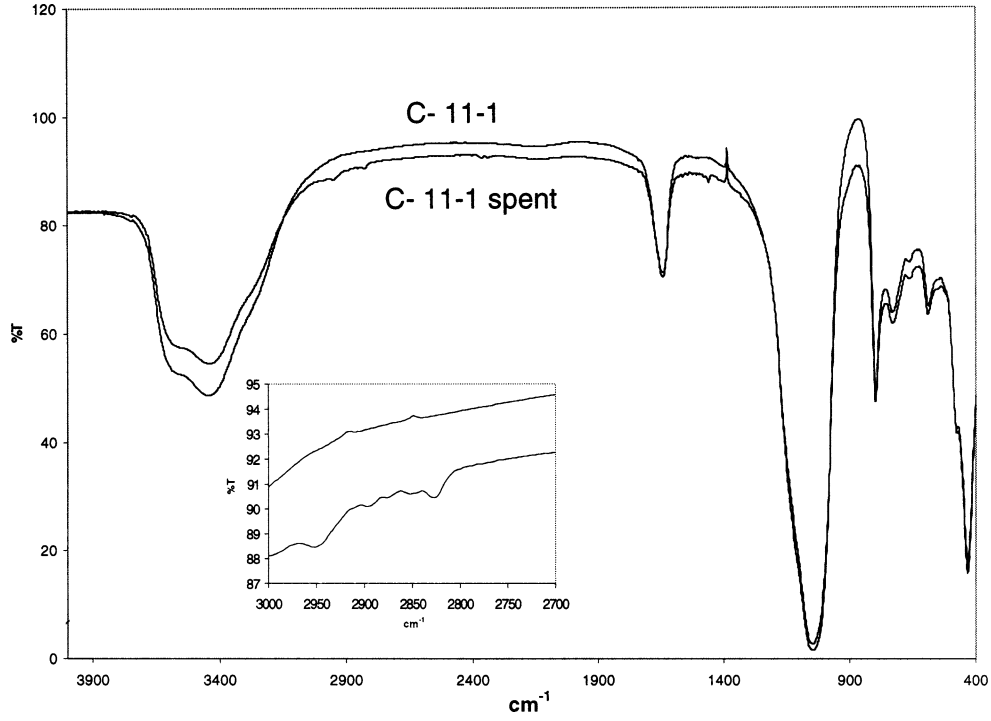

Fig. 5. FTIR C-11-1 before and after reaction (spent).

Catalyst 20 had less activity than catalysts 18 and 19, and after approximately 100 min, some variations in the conversion of aniline were observed.

The conversion of aniline on LTL took more time to increase than for catalysts 18, 19, and 20. At approximately 200 min, a maximum in conversion is observed, and then the catalyst starts to deactivate. The smallest conversion was observed when catalyst 11-1 was used. Catalyst 11-1 was deactivated in a very short period of time.

4. Discussion

4.1. Characteristics of cocrystallized RHO–zeolite X (FAU) and zeolite LTL

Zeolite RHO with different SiO_2/Al_2O_3 ratios was synthesized. EDX data show that this ratio increased when the initial batch composition had a higher SiO_2 content, as confirmed by FTIR. The band around 700–800 cm^{-1} shows a

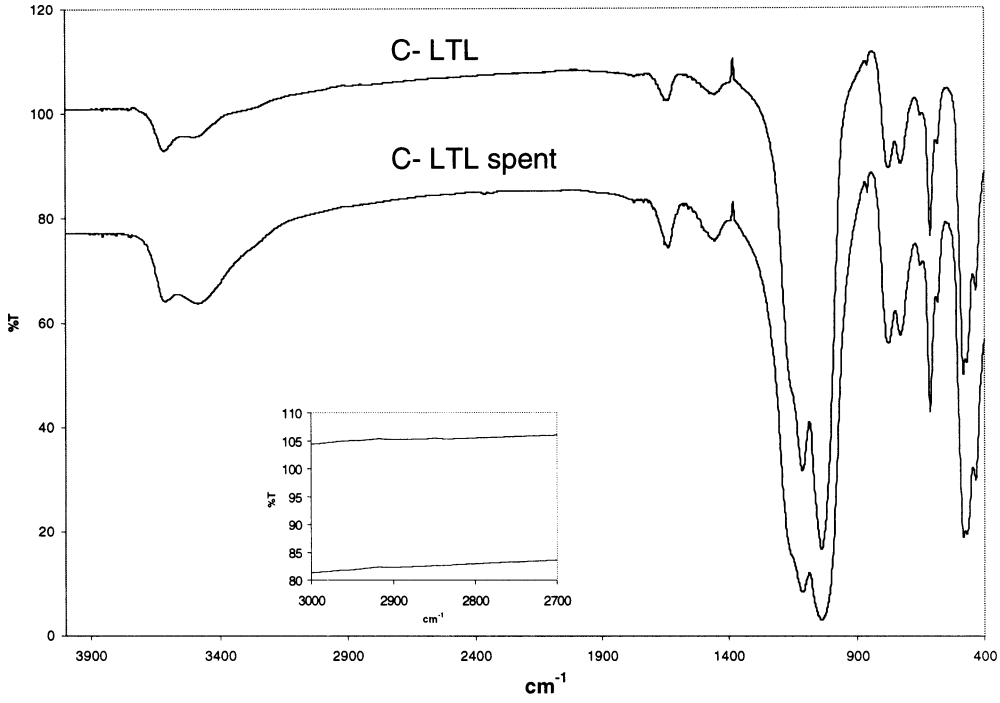

Fig. 6. FTIR C-LTL before and after reaction (spent).

Table 4
Aniline adsorption

Catalyst	X_m (μmol/g)	Acid site concentration (μmol/m^2)
C-18	54.00	0.585
C-19	11.31	0.161
C-20	3.15	0.125
C-11-1	5.78	0.336
C-LTL	12.68	0.060

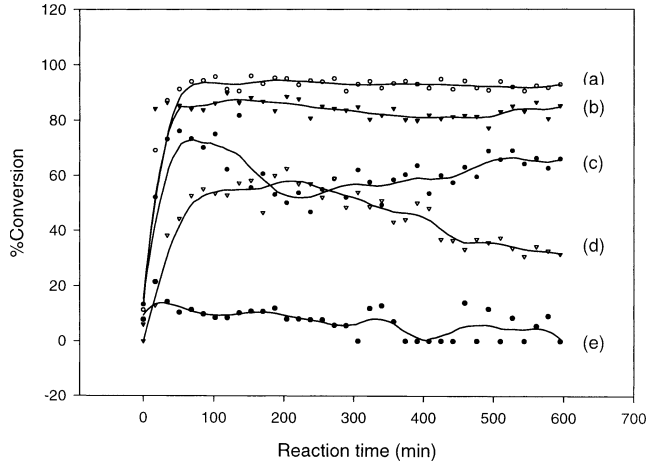

Fig. 7. Conversion based on aniline at 400 °C as a function of time on stream for (a) C-18, (b) C-19, (c) C-20, (d) C-LTL, and (e) C-11-1.

shift that is normally observed when the SiO_2/Al_2O_3 ratio is modified [17]. The EDX SiO_2/Al_2O_3 ratios for zeolite RHO samples (labeled C-11-1 and C-18) are very close, and for samples labeled C-19 and C-20 they are also comparable. This result is in agreement with the FTIR shift observed in Fig. 4. When the ratio of SiO_2/Al_2O_3 increased for the initial batch composition, the particle sizes of the final products increased. SEM data show that the particle sizes of sample C-11-1 and C-18 are smaller than particle sizes of C-19 and C-20. This phenomena is commonly observed in the synthesis of zeolites. Smaller particles are obtained for larger Al content. The partial isomorphous substitution of silicon by other tetrahedron-forming elements can influence crystal size [19].

Faujasite appeared as a cocrystallizing phase when small concentrations of Cs were used in the synthesis of zeolite RHO [11]. The concentration of Cs used in all the experiments was the same, but due to the increase in viscosity observed when smaller amounts of colloidal silica solutions were used, the homogeneous distribution of Cs ions in the system is more difficult to achieve, and some Faujasite is then obtained. Excess silica acts as a diluent for the gel and less viscosity is observed when the amount of colloidal silica is increased. Cs is more evenly distributed and less Faujasite is formed. Zeolite X (FAU) is the preferred product when experiments are performed without Cs and using the same batch composition. Faujasite X is produced when a small SiO_2/Al_2O_3 ratio is used. Faujasite Y is the product formed for higher SiO_2/Al_2O_3 ratios [20]. The most intense peak for Faujasite is observed by XRD but its intensity compared to the peaks of zeolite RHO is very small. The maximum FAU/RHO ratio was obtained in C-18 around 0.2. The main phase observed by SEM corresponds to zeolite RHO.

Smaller particles with a different shape must be due to zeolite X (FAU). Zeolite X (FAU) particles are smaller and

disc like when Cs was used. The particles are around 1 μm and spherical when Cs is not used.

Zeolite RHO is characterized by a high framework flexibility [21]. The framework of zeolite RHO becomes distorted and a different diffraction pattern is observed when the zeolite is dehydrated. All of the samples prepared were observed dehydrated under the same conditions. Zeolite RHO materials (labeled C-20) with the highest Si/Al ratios after dehydration show characteristics peaks of the hydrated phase. Dehydration of the zeolite is more difficult to achieve under the same conditions when the Si/Al ratio is increased and a less flexible framework is obtained.

The surface area measured for sample C-11-1, pure zeolite RHO, is the smallest of all the samples. Under the pretreatment conditions, the framework of zeolite RHO is distorted leading to modification of the pore openings. As a result the measured surface area is less than expected for a zeolite with a pore opening of 8-membered rings. This behavior for zeolite RHO has been previously reported [22,23]. The median pore diameter of C-11-1 obtained after BET analysis is very high (Table 3) and should correspond to macropores due to crystal imperfections and not to internal pores. Imperfections in the surface of C-11-1 are seen in the SEM micrograph for this sample in Fig. 3.

4.2. Discussion of catalytic results

The mechanism of aniline methylation over basic zeolite Y was reported by Ivanova using ^{13}C MAS NMR [24]. Under basic conditions aniline is not strongly adsorbed on the surface due to methanol adsorption. Aniline is associated with Lewis acid sites (cations) of the catalyst while methanol is strongly adsorbed on basic sites (framework oxygen). Ivanova et al. [24] proposed that after heating the reaction system, methanol is dehydrogenated in basic zeolites, forming very reactive formaldehyde, which can alkylate aniline. At low surface coverage with aniline, alkylation competes with side reactions leading to surface formate species that could be responsible for fast deactivation of basic catalysts [21,25].

N,N-dimethylation of aniline to produce NNDMA with X and Y zeolites exchanged with Li, Na, K, Rb, and Cs does not occur in the case of zeolites Y [10]. The more basic zeolite X favors N-methylation to NMA as well as to N,N-dimethylation product. In the case of N,N-dimethylation stronger basic sites are required than for C-alkylation [10]. In our reactions N,N-dimethylation occurs with cocrystallized RHO–zeolite X (FAU) and the catalyst is still active over a period of 10 h after which we stopped the reaction. This result may be due to the high basicity of the cocrystallized zeolites. The Si/Al ratio (EDX) for the catalysts labeled in this work as C-20, C-19, C-18, C-11-1, and LTL is such that we have an order of Si/Al of LTL > 20 > 19 > 18 > 11-1. From this result, we expect basicity of the prepared materials to increase in the order LTL < 20 < 19 < 18 < 11-1. The activity of the cocrystallized RHO–zeolite X (FAU) material in terms of production of NNDMA (Fig. 7) agrees with a larger number of expected basic sites for C-18 as compared to catalysts 19 and 20. The beneficial effect of cocrystallization is confirmed by the fact that the less active catalyst in these series is C-11-1, which is the one that corresponds to pure zeolite RHO. Activity decreases rapidly for pure RHO as compared to activity of the other materials as seen in data of Fig. 7.

The percentage of conversion of aniline is directly related to the presence of zeolite X (FAU). The catalyst that had the highest FAU/RHO ratio also produced the highest conversion (C-18). The conversion of aniline was the lowest (C-11-1) when no zeolite X (FAU) was detected by XRD or SEM. However, C-11-1 still has some activity.

Pure alkaline zeolite X has been reported as the best catalyst for the selective production of NNDMA with high aniline conversion but deactivates very soon [10,26]. Using cocrystallized zeolite RHO–zeolite X (FAU), high conversion, selectivity to NNDMA, and no deactivation were observed after 10 h of reaction. The more active phase (zeolite X) when more dispersed may produce active sites that are not very concentrated. For C-18, with the smallest particle size, less deactivation and high conversion were observed. Catalyst effectiveness is larger for smaller crystals. Coke deactivation can be more severe for larger crystals [19]. Larger pore size zeolites like zeolite X and zeolite Y are susceptible to deactivation by coke, because the mixture of high molecular weight aromatic compounds formed in the supercages of the zeolite may be trapped, being too large to diffuse out through the smaller apertures [20]. For smaller particles, the diffusion of compounds is easier and less deactivation should be expected [19]. Different diffusion rates of reactants and products inside the catalysts due to the differences in their crystal size may also explain differences in the observed lag times.

Zeolite RHO may block the large openings in zeolite X, decreasing the possibility of forming coke inside the channels of zeolite X. This kind of phenomenon was observed for a mixture of synthetic offretite and erionite. In these mixed systems erionite blocked the pores of offretite and good selectivity was observed [27].

The conversion of aniline over catalyst 11-1 was the lowest among all the catalysts tested. The pores of zeolite RHO are very small (3.6 Å) and aniline can not get inside. The outer surface of RHO is available for the reaction and has a much smaller surface area than internal sites. Aniline can be adsorbed on the surface of pure zeolite RHO (Table 4) but the coverage is very small. Some conversion for RHO can be obtained; however, high deactivation occurs because there is not enough aniline available to react with all the formaldehyde produced by dehydrogenation of methanol on zeolite RHO. The FTIR of spent catalyst 11-1 (Fig. 5) shows evidence of $-CH_2$ bands. Perhaps this catalyst is deactivated by the formation of surface formate.

Cesium cations act as templates for the synthesis of zeolite RHO [12]. Faujasite instead of zeolite RHO is

obtained in the absence of cesium. In addition to being an important cation for the cocrystallization of zeolite RHO–zeolite X, cesium is also important since cesium creates stronger basic sites than any other alkali metal [28]. The production of NNDMA is favored by very strong basic sites and by an excess of methanol [26].

For cocrystallized zeolites, methanol reacts very easily with zeolite RHO producing formaldehyde and aniline is adsorbed on zeolite X (FAU). Both zeolites have an important role in the aniline methylation reaction.

Zeolites Na-L (LTL) and K-L (LTL) have been studied in aniline methylation [25] and are selective toward N-methylation. The more basic K-L is more active than Na-L, but both deactivate in less than 400 min. The maximum conversion [25] was around 30% when using K-L. Zeolite K,Sr-LTL gave a conversion around 60% (see Fig. 7). This increase could be due to the lower Si/Al ratio of the zeolite reported here. This zeolite also does not have any sodium ions, but has more potassium and also strontium, making it a more basic zeolite [28].

LTL does not adsorb aromatics in the 12R window [25]. A molecular effect may control the adsorption. Such molecular effects could be responsible for the low adsorption of aniline (Table 4) observed in these experiments. Zeolite K,Sr-LTL has the highest surface area but does not adsorb as much aniline as C-18 (RHO/zeolite X) that readily adsorbs aniline, but has a lower surface area than LTL. A high surface area does not guarantee high conversion in this reaction. The basicity and aniline adsorption of the catalyst are more important than surface area. Cocrystallized zeolite RHO–zeolite X is more basic than zeolite L, because the ratio Si/Al in cocrystallized zeolites is lower than that for LTL (Table 2) and cesium cations present in cocrystallized zeolites can create stronger basic sites than strontium and potassium [28]. Adsorption of aniline in LTL is lower than in cocrystallized C-18. Zeolite LTL does not adsorb aromatics in the 12-membered ring window [25]. In the same report the authors compared the activity of pure zeolite Na-X with Na-L and showed that Na-X is much more active than Na-L. Comparing zeolites with different structures, aluminum contents, and types and amounts of cations present is very difficult. The only similarity between LTL and FAU is that both of these materials have openings of 12-membered rings.

Catalytic studies using cocrystallized zeolite RHO–zeolite X for periods of time longer than 10 h are required to determine the maximum operation time of this system. Long-term studies are also important for studying the deactivation mechanism and possible regeneration of the catalyst.

5. Conclusions

The alkylation of aniline with methanol was attempted over various cocrystallized RHO–zeolite X (FAU) catalysts and over a zeolite LTL catalyst. The cocrystallized RHO–zeolite X (FAU) as well as the LTL catalyst are active in the N-dialkylation of aniline with methanol. Pure zeolite RHO was found to be less active. No C-alkylation product was observed. For cocrystallized zeolites, the conversion is related to the presence of zeolite X (FAU). Constant activity for this reaction can be maintained under conditions studied for the cocrystallized catalyst. Higher aniline conversion than previously reported was obtained when K,Sr-LTL was used instead of Na- or K-LTL.

A synergistic effect of cocrystallized zeolite RHO–zeolite X was observed. Zeolite X allowed a high conversion of aniline due to strong adsorption of aniline. Zeolite RHO provided high dispersion of zeolite X (active sites for aniline adsorption) and high activation of methanol to produce high selectivity toward NNDMA, high aniline conversion, and high activities for longer periods of time than those reported for pure zeolite X.

Acknowledgments

We acknowledge support from the Geosciences and Bioscience Division, Office of Basic Energy Sciences, Office of Science, U.S. Department of Energy for catalytic work, and NASA/CAMMP for synthesis of zeolites. We also thank Dr. Francis S. Galasso for helpful discussions.

References

[1] I. Ivanova, E. Pomakhina, A. Rebrov, M. Hunger, Y. Kolyagin, J. Weitkamp, J. Catal. 203 (2001) 375.
[2] J. Santhanalakshmi, R. Thirumalaiswamy, Appl. Catal. A: Gen. 147 (1996) 69.
[3] P.Y. Chen, M.C. Chen, H.Y. Chu, N.S. Chang, T.K. Chuang, Stud. Surf. Sci. Catal. 28 (1986) 739.
[4] S.P. Elangovan, C. Kannan, B. Arabindoo, V. Marugesan, Appl. Catal. A: Gen. 174 (1998) 213.
[5] J.M. Campelo, A. Garcia, D. Luna, J.M. Marinas, A.A. Romero, J.J. Toledano, Stud. Surf. Sci. Catal. 135 (2001) 4137.
[6] A.-N. Ko, C.-L. Yang, W.-D. Zhu, H.-E. Lin, Appl. Catal. A: Gen. 134 (1996) 52.
[7] V. Krishnasamy, V. Murugesan, Ind. J. Chem., Sect. A 34A (1995) 469.
[8] Y.K. Park, K.Y. Park, S. Woo, Catal. Lett. 26 (1994) 169.
[9] N. Takayima, Y. Koinuma, K. Ando, S. Murai, Nippon Kagaku Kaishi 11 (1979) 1453.
[10] B. Lian Su, D. Barthomeuf, Appl. Catal. A: Gen. 124 (1995) 73.
[11] H. Robson, D. Shoemaker, R. Gilvie, P. Manor, in: W.M. Meier, J. Uytterhoeven (Eds.), Molecular Sieves. Advances in Chemistry Series, Vol. 12, Am. Chem. Society, Washington, DC, 1973, p. 106.
[12] J.M. Newsam, D.E.W. Vaughan, K. Strohmaier, J. Phys. Chem. 99 (1995) 9924.
[13] R.D. Shannon, M. Keane, L. Abrams, R.H. Staley, T.E. Gier, D.R. Corbin, G.C. Sonnichsen, J. Catal. 113 (1988) 367.
[14] J.M. Marinas, C. Jimenez, J.M. Campelo, M.A. Aramendia, V. Borau, D. Luna, Simp. Iberoam. Catal. [Trab] 7 (1980) 79.
[15] P.C. Russell, S.L. Stuhler, A.L. Kouli, J. Warzywoda, A. Sacco Jr., Stud. Surf. Sci. Catal. 135 (2001) 295.
[16] M. Park, S.H. Kim, N.H. Heo, S. Komarneni, J. Porous Mater. 3 (1996) 151.

[17] W.H. Flank, ACS Symp. Ser. 40 (1977) 43.
[18] C. Poole, S. Poole, in: Chromatography Today, Elsevier, Amsterdam, 1997, p. 92.
[19] F. Di Renzo, Catal. Today 41 (1998) 37.
[20] B. Gates, Catalytic Chemistry, Wiley, New York, 1992.
[21] J. Parise, T. Gier, D. Corbin, D. Cox, J. Phys. Chem. 88 (1984) 1635.
[22] D.R. Corbin, L. Abrams, G.A. Jones, M.M. Eddy, W.T.A. Harrison, G.D. Stucky, D.E. Cox, J. Am. Chem. Soc. 112 (1990) 4821.
[23] L. Abrams, D.R. Corbin, J. Catal. 127 (1991) 9.
[24] I. Ivanova, E. Pomakhina, A. Rebrov, Stud. Surf. Sci. Catal. 135 (2001) 8.
[25] B. Lian Su, D. Barthomeuf, Appl. Catal. A: Gen. 124 (1995) 81.
[26] M.A. Aramendia, V. Borau, C. Jimenez, J.M. Marinas, F.J. Romero, Appl. Catal. A: Gen. 183 (1999) 73.
[27] K. Minachev, Y.A. Isakov, in: W.M. Meier, J. Uytterhoeven (Eds.), Molecular Sieves. Advances in Chemistry Series, Vol. 12, Am. Chem. Society, Washington, DC, 1973, p. 454.
[28] R. Deka, R. Roy, K. Hirao, Chem. Phys. Lett. 332 (2000) 576.